SpiroSurface: A Repulsive and Attractive Force Display for Interactive Tabletops Using a Pneumatic System

Taku Hachisu
University of Tsukuba and Microsoft Research

Masaaki Fukumoto
Microsoft Research

We present SpiroSurface, a novel force display for interactive tabletops. SpiroSurface uses a pneumatic system to generate both repulsive and attractive forces. We develop a prototype with 5x5 grid holes on the surface connected to an air compressor and vacuum tanks through electromagnetic valves. The display can output a maximum of +1.0 and -0.08 megapascal (MPa) pressure from a hole that generates 74 and -6 N force. We investigated the latency of the output pressure through pneumatics and an experiment, which indicated a minimum of 50-ms latency. The display allows the creation of three kinds of novel interactions: (1) enhancement of GUI, (2) deformation of soft objects, and (3) three degrees of freedom rotation of objects. In the first application, users can feel the force from the display without holding or attaching additional devices. In the second and third applications, the shape and motion of an object on the surface can be manipulated without embedding additional active components in the objects. These aspects allow users to easily experience interaction and expand the freedom of interaction design. We introduce several examples combining video projection and motion tracking. These examples demonstrate the potential of the display.

Published by the IEEE Computer Society
0272-1716/18/$33.00 ©2018 IEEE

Researchers in the field of human-computer interaction have explored various interactions on tabletops. Users interact with physical or virtual widgets on a surface that represents output from a computer and input from users through different modalities. Force displays enrich the interaction by directly or indirectly representing the event on the surface. Several methods for generating force have been developed, such as using air pressure,[1,2] magnetic force,[3,4] and mechanical actuators[5] embedded in the surface or in physical gadgets. (See the "Background and Related Work" sidebar.)

This work addresses two challenges for facilitating novel interaction on tabletop surfaces using a force display. One is embedding the force supply into the surface; several existing force display systems embed actuators in a physical widget or allow the user to attach components. This environmental force supply enables users to easily experience interaction without holding or attaching additional devices. Furthermore, because physical widgets can move or deform when receiving force directly from the surface, an environmental force supply allows for the reduction of active mechanical and electrical components in the physical widget. Further, communication between the widgets and the host computer is not always required. The other challenge is supplying force in more than one direction. Existing force displays for interactive tabletops can be classified into three categories in terms of direction of actuation from the surface to the object: lateral, repulsive, or attractive. Because each direction has advantages for different purposes, a display that can supply force in more than one direction expands the freedom of interaction design. We are unaware of a display satisfying our two challenges.

We previously developed VacuumTouch, which offers a direct touch interaction that provides an attractive force on the surface in an interactive tabletop setup.[6] The surface has grid holes connected to a vacuum tank through electromagnetic air valves, which allows users to experience the interaction on the surface without holding or attaching additional devices. Although we demonstrated the potential of an attractive force feedback system, repulsive force feedback systems continue to have an inherent advantage. In the case of adding haptic feedback to a virtual button on a surface, for example, attractive force can recommend the button by encouraging the fingers to press it, whereas repulsive force can warn users to not press it by rejecting the fingers.

In this article, we present a novel force display for interactive tabletops, SpiroSurface, which provides both repulsive and attractive forces by extending the architecture of VacuumTouch. SpiroSurface employs two air tanks—one for attractive and the other for repulsive forces—connected to holes on the surface through electromagnetic air valves. A microcontroller controls the valves according to the user's input, which realizes the force display for the interactive tabletop. The contributions of the proposed work are: (1) the implementation of a force display; (2) quantitative evaluation of a force display; and (3) demonstrations of several examples of applications of SpiroSurface, including direct touch haptic interaction, control of object shape, and control of 3D object rotation. Finally, we discuss the advantages and disadvantages of the current implementations and limitations of our approach.

SPIROSURFACE

In this section, we describe the implementation of SpiroSurface. Depending on the application, the display can be combined with a tabletop interface setup, such as a video projector and motion tracking sensors.

Architecture

To build a display that provides both repulsive and attractive forces for interactive surfaces, we developed a prototype of SpiroSurface consisting of an air compressor (Taizhou Outstanding Industry and Trade Co., Ltd., ZBM-0.067/8), an air vacuum pump (Sato Vac Inc., ODF-50W), a 5.5-liter iron air compressor tank ($Tank_{com}$), a 5.5-liter iron air vacuum tank ($Tank_{vac}$), two arrays of 25 (5x5) electromagnetic air valves (Amico, VX2120-X64, DC12V (10.2 W), normally closed), 25 y-shape connectors, a surface made of acrylonitrile butadiene styrene (ABS) resin with 25 (5x5) holes, and a microcontroller (NXP semiconductors, mbed LPC1768), as illustrated in the left image of Figure 1. Each tank was connected to the appropriate pump (compressor and

vacuum) through an air tube. Each tank had an analog air pressure gauge. An air regulator was installed on $Tank_{com}$ to adjust the air pressure from 0 to +1.0 MPa (all units of pressure in this article refer to gauge pressure); $Tank_{vac}$ was set at either 0 or -0.08 MPa. Twenty-five holes on each tank, thus 50 holes, were connected to 25 y-shape connectors through tubes and valves. The other sides of the y-shape connectors were connected to the holes on the surface. The diameter of the holes was 9.728 mm, designed to be properly covered by the tip of a finger. The size of the surface was 280x220 mm, as indicated in the right image of Figure 1.

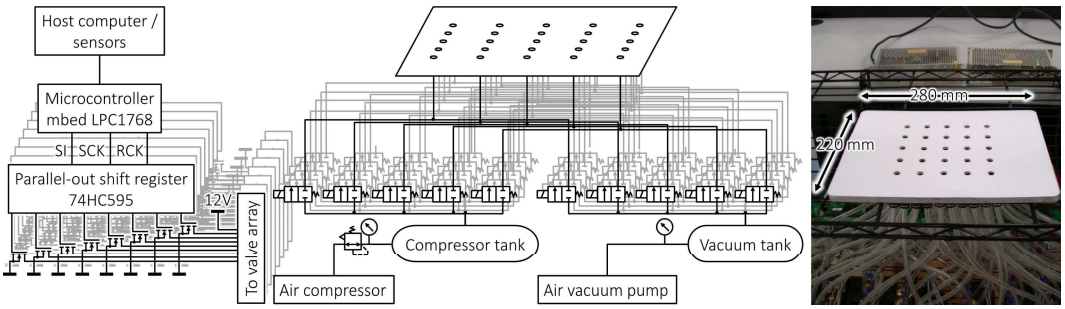

Figure 1. (left) SpiroSurface consisting of an air compressor, an air vacuum pump, two 5.5-liter iron air tanks, 50 electromagnetic air valves, 25 y-shape connectors, and a surface with 25 holes. The air valves are controlled by a microcomputer through parallel-out shift registers and field effect transistors (FETs). (right) Surface of SpiroSurface (280x220 mm).

Valve array switching was controlled by a microcontroller through parallel-out shift resisters (Toshiba, 74HC595) using a serial peripheral interface (SPI) and FETs. The clock frequency of the SPI was set at 20 MHz, and the microcontroller updated the open/close condition of the valves with a 1-ms loop.

Capability

Force

Theoretically, the pressure on the holes becomes equal to that of the tank while the valves are open and the holes are completely covered with objects or by users. The maximum pressure capacities of $Tank_{com}$ and $Tank_{vac}$ were +1.0 MPa and -0.08 MPa, respectively. When one hole is open, the maximum generated repulsive and attractive forces are theoretically approximately 74 and –6 N, respectively.

While the valves are open and the holes are not covered, the absolute air pressure falls and becomes a static state where the amount of the air supplied by the air compressor or vacuum pump becomes equal to that emitted into the atmosphere. As the number of opened and uncovered holes increases, the pressure declines progressively, because the flow passage area increases. Thus, the system must avoid opening the holes for long periods to maintain high pressure.

Latency

We evaluated the latency of the generation and dissipation of the pressure. We define the latency as the time delay between the microcontroller's order and attaining the expected air pressure. We consider that studying the latency of the developed device offers two suggestions for designing human-computer interactions. One relates to how fast the display can react to a user's input. Since Ferrell recognized that haptic feedback latency adversely influences the user's performance,[7] researchers have investigated the relationships between latency and user experience. Although there is considerable literature and the values vary depending on the task, the less-than-100-ms latency is perceived by human users and is sufficient to reduce the user experience. The other suggestion relates to the possibility of controlling the force's intensity. Although the developed display employs on-off control, it could control the force's intensity using a pulse width

modulation (PWM) scheme if it could control the duration of the opening and closing time of the valves on the order of milliseconds or less. Although this section describes the evaluation of the developed display and some guidelines, a quantitative user study is out of the scope of this work.

Latency theory

Latency is expected to depend significantly on the activation time of the electromagnet in the valve (t_{valve}) and the travel time of the air to attain the target air pressure on the hole on the surface (t_{air}). Although the microcontroller can activate and deactivate all FETs in less than 1 ms, the valve requires time to open/close a nozzle by moving a poppet using electromagnetic and spring force. The general valve's response time from fully closed to fully open or *vice versa* under no pressure is 10-100 ms. However, when high pressure is applied to the inlet or outlet, the closing and opening times are decreased and increased, respectively.[8] This is because the pressure force helps the valve open the poppet, whereas it impedes the closing movement of the poppet. Therefore, the reaction time corresponding to the pressure is not in the datasheet and must be measured for evaluating the latency.

Conversely, t_{air} can be expressed as

$$t_{air} = \frac{Q}{V} \tag{1}$$

where V is the volume of the travel path and Q is the flow rate. The travel path for one hole consists of two air tubes connected to a y-shape connector. We approximate the air tubes as one cylindrical path with radius r (5.0 mm) and length l (80 cm). Thus, V can be calculated by

$$V = \pi r^2 l. \tag{2}$$

According to the Hagen-Poiseuille equation, Q can be expressed as

$$Q = \frac{\pi r^4}{8} \cdot \frac{\Delta p}{\eta l}, \tag{3}$$

where Δp is the pressure gradient and η (1.822 × 10-5 Pa · s) is the dynamic viscosity of air at 20 degrees Celsius. By substituting Equations 2 and 3 into Equation 1, t_{air} can be calculated by

$$t_{air} = \frac{8\eta l^2}{r^2 \Delta p}. \tag{4}$$

Although we calculated t_{air} with Δp 0.08 to 0.2 MPa, which is the pressure range used in the following experiment and application, the value is negligibly small (less than 1 ms) compared to t_{valve} (more than 10 ms).

Latency experiment

We measured the temporal profiles of the air pressure under three conditions: (1) generation of pressure, (2) dissipation of pressure with a hole open to the atmosphere, and (3) dissipation of pressure with a hole open to the other air tank. The measurement system consisted of SpiroSurface, a metal cap with an air pressure sensor (Metrodyne Microsystem, MIS-2503-150G and MIS-2503-015V), and an oscilloscope, as indicated in the left image of Figure 2. One hole on the surface is covered with the metal cap, which is sealed with tape and glue to prevent air leaking. The hole is connected to two valves (Valve1 and Valve2). Valve1 is connected to either Tank_{com} or Tank_{vac}; Valve2 is connected to the atmosphere under Conditions 1 and 2 and to either Tank_{vac} or Tank_{com} under Condition 3. The oscilloscope monitored voltages of the digital output pin of the microcontroller and the signal output pin of the pressure sensor.

Table 1 displays all pairs of the air pressure applied to Valve1 P_{Valve1} and Valve2 P_{Valve2} from the tanks or the atmosphere before beginning measurement under the three conditions. Under Condition 1 (generation of pressure), we first closed the two valves. Thus, P_{Valve1} was equal to that of Tank_{com} or Tank_{vac}, and P_{Valve2} was 0.0 MPa, as indicated in the right image of Figure 2 (Condi-

tion 1). Thus, the microcontroller set the digital output pin low. Then, the microcontroller simultaneously ordered Valve1 to open and set the digital output pin high, triggering the oscilloscope to begin recording voltage from the air pressure sensor, as indicated in the right image of Figure 2 (Condition 1). We conducted this measurement with (P_{Valve1}, P_{Valve2}) {(-0.08, 0.00), (+0.08, 0.00), (+0.10, 0.00), and (+0.20, 0.00)} MPa.

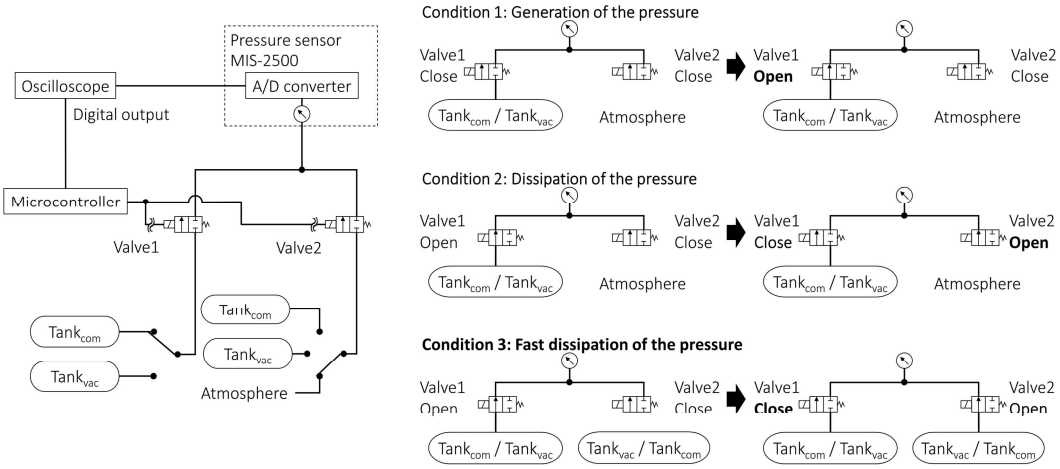

Figure 2. (left) Illustration of latency measurement system. (right) Illustration of three conditions for latency measurement: Condition 1 - generation of pressure, Condition 2 - dissipation of pressure with a hole open to the atmosphere (dissipation of pressure), and Condition 3 - dissipation of pressure with a hole open to the other air tank (fast dissipation of pressure).

Table 1. Pairs of air pressure (P_{Valve1}, P_{Valve2}) applied to Valve1 and Valve2 from $Tank_{com}$, $Tank_{vac}$, or the atmosphere under the three conditions.

	(P_{Valve1}, P_{Valve2}) expressed in MPa
Condition 1: Generation of pressure	{(+0.2, 0), (+0.1, 0), (+0.08, 0), (-0.08, 0)}
Condition 2: Dissipation of pressure	{(+0.2, 0), (+0.1, 0), (+0.08, 0), (-0.08, 0)}
Condition 3: Fast dissipation of pressure	{ (+0.08, -0.08), (-0.08, +0.08)}

Under Condition 2 (dissipation of pressure), we used the same setup. As indicated in the right image of Figure 2 (Condition 2), the microcontroller ordered Valve1 to open and set the digital output pin low. After several seconds, the microcontroller simultaneously ordered Valve1 to close and Valve2 to open, and set the digital output pin high, which triggered the oscilloscope to begin recording the voltage. We conducted this measurement with (P_{Valve1}, P_{Valve2}) {(-0.08, 0.00), (+0.08, 0.00), (+0.10, 0.00), and (+0.20, 0.00)} MPa.

Under Condition 3 (fast dissipation of pressure), we modified the setup as illustrated in the right image of Figure 2 (Condition 3), where Valve2 was connected to $Tank_{vac}$ or $Tank_{com}$. The microcontroller ordered Valve1 to open and set the digital output pin low. After several seconds, the microcontroller simultaneously ordered Valve2 to open and set the digital output pin high, triggering the oscilloscope to begin recording the voltage. We conducted the measurement with (P_{Valve1}, P_{Valve2}) {(-0.08, +0.08) and (+0.08, -0.08)} MPa. In this case, the dissipating negative and positive pressure are labeled as -0.08 MPa' and +0.08 MPa' to differentiate them from those in Condition 2.

The left image of Figure 3 displays the temporal profiles of air pressure generation (Condition 1). The profiles of all conditions are similar regardless of the air pressure. After the microcontroller sent a signal to open Valve2, the air pressure did not change for approximately 10 ms. This is considered the time required for initiating the operation to move the poppet to open

Valve1. Then, it required approximately 50 ms for the air pressure to become static. This is considered the travel time of the poppet.

The right image of Figure 3 displays the temporal profiles of the dissipation of air pressure (Conditions 2 and 3). The profile of dissipating pressure with a hole open to the atmosphere in Condition 2 is different from that of dissipating pressure with a hole open to the other air tank in Condition 3. In Condition 2, after the microcontroller sent the signal, the air pressure does not change for approximately 50 ms. In this phase, Valve2 may open before Valve1 begins to close, where Valve1 supplies the pressure from Tank1 while Valve2 exhausts the pressure to the atmosphere. Thus, the pressure does not change. Then, it requires approximately 400 ms for the air pressure to become static (same as the atmosphere). In this phase, the poppet of Valve1 can be moving to close Valve1. However, the pressure requires a greater time to become static than in Condition 1. This could be because closing the valve requires more time than opening the valve under high pressure, as mentioned earlier. Condition 3 indicates inverted profiles compared to Condition 1. When Valve2 opened, Tank_{com} connected to Tank_{vac}, where the air pressure goes to 0.0 MPa (the average of P_{Valve1} and P_{Valve2}). The results indicate that the latency of dissipating pressure can be reduced to approximately 50 ms.

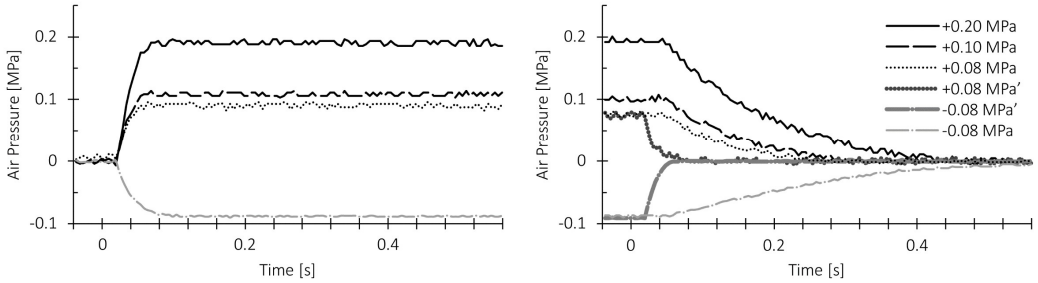

Figure 3. Time delay between the microcontroller's order and attaining the expected air pressure. (left) Generation of pressure requires approximately 60 ms after the microcontroller orders the valve to open (Condition 1). (right) Dissipation of pressure requires approximately 450 ms when the hole is open to the atmosphere (Condition 2), whereas it requires 50 ms when the hole is open to the other tank (Condition 3).

Before all measurements, we manually set the air pressure in the tanks by adjusting the regulator and monitoring the analog gauge on the tanks. However, the air pressure measured by the pressure sensor was slightly different from the one indicated by the analog air pressure gauge. This could be due to pressure drop and the inherent error of the air gauge and pressure sensor.

In summary, the developed display can output pressure with approximately 50- to 400-ms latency. Users could perceive the latency, especially during sensitive interaction such as direct touch interaction. In informal tests, we confirmed that human users could easily perceive the latency during the direct touch interaction, although the latency did not adversely influence the performance of a certain GUI task. Moreover, it is difficult for the display to employ the PWM scheme to control the force's intensity. A solution to achieving faster reaction times would be to use faster solenoid valves. Currently, solenoid valves with less than 1-ms reaction time are available. Employing servo valves or proportional valves is another option, although the hardware and software of the control unit could require modification.

APPLICATIONS

In this section, we describe several applications of SpiroSurface. The challenges are (1) not having users hold or attach additional devices for experiencing interaction, (2) deforming and moving objects without embedding active components in the object, and (3) providing force to two directions (repulsive and attractive directions). These challenges address three kinds of novel human-computer interactions: (1) enhancement of the GUI, (2) deformation of a soft object, and (3) three degrees of freedom (DoF) rotation of an object. Furthermore, this section introduces a

quantitative evaluation of one of the enhanced GUIs, which was conducted to study the capability of the developed force display in our previous work.[6] Because it is difficult to study the user experience in other applications in a quantitative manner, the video illustrates live demonstrations of these applications (https://youtu.be/SqfEaby3Mj4).

Enhancement of the GUI

We applied SpiroSurface to enhance the GUI because assessing the usability of the GUIs allowed us to evaluate the system. We developed three types of GUI, namely SpiroButton, SuctionSlider, and SuctionDial.

To develop the tabletop touch screen, we set the scanning range finder (Hokuyo Automatic, URG-04LX-UG01) and capacitance sensor (single electrode) to measure the 2D position of a finger on the surface and detect finger contact with the surface, respectively (see the top image of Figure 4). The projector (BenQ, MS 616ST) was installed above the surface. First, the touch sensor measures the user's touch event and sends it to the computer. Then, the computer processes the event and outputs the visual image and control signal for the valve array to the projector and the microcontroller, respectively. The touch sensor can be compatible with other input technology of similar capability, such as a camera vision or infrared grid touch sensor.

SpiroButton

The middle image of Figure 4 displays an example of the SpiroButton, where the system is asking whether the user really wants to delete an important file (such as a system file) by asking "Yes" or "No." The user must press and hold the button for two seconds to select the input. That is, the user is able to cancel the selection within two seconds by releasing his or her finger from the surface. Because the system knows how important the file is, it recommends not deleting it. Thus, the system provides a repulsive force at the hole on the "Yes" button and provides an attractive force at the hole on the "No" button. Consequently, the user intuitively knows what button is recommended by the system.

SuctionSlider

The bottom-left image of Figure 4 displays an example of SuctionSlider, where the user is browsing a document. The user is reading the document while scrolling with the slider bars on the right and bottom. The user's attention is on the contents of the document, rather than on the slider bars. Thus, it is possible that the user could attempt to scroll through a document even when it comes to the end or edge. SuctionSlider addresses this issue by forcibly stopping the user's finger on the slider. This results in intuitive haptic cues as if the slider physically contacted the end.

SuctionDial

The dial menu interface is used in a number of touch screen applications such as alarms. One of the issues for this interface is that it is difficult to identify the end of the dial. As seen in existing methods, a visual spring effect is provided at the end of the dial, where the dial can continue to be scrolled in the same direction after the end has been reached and returns to the end when the finger is released. However, it is impossible for this to occur with a physical dial. To simulate a realistic dial menu interface, we created SuctionDial, as illustrated in the bottom-right image of Figure 4. SpiroSurface provides a suction force at the end of the dial, where a user physically cannot continue to scroll the dial in the same direction.

Evaluation

We conducted an experiment to study the attractive force feedback provided by the display. The task of the experiment was to identify the end of the dial GUI. The task allowed us to quantita-

tively evaluate the usability of the attractive force as an interface and compare it with the existing technique. This experiment was conducted in our previous work, which includes the details of the setup.[6]

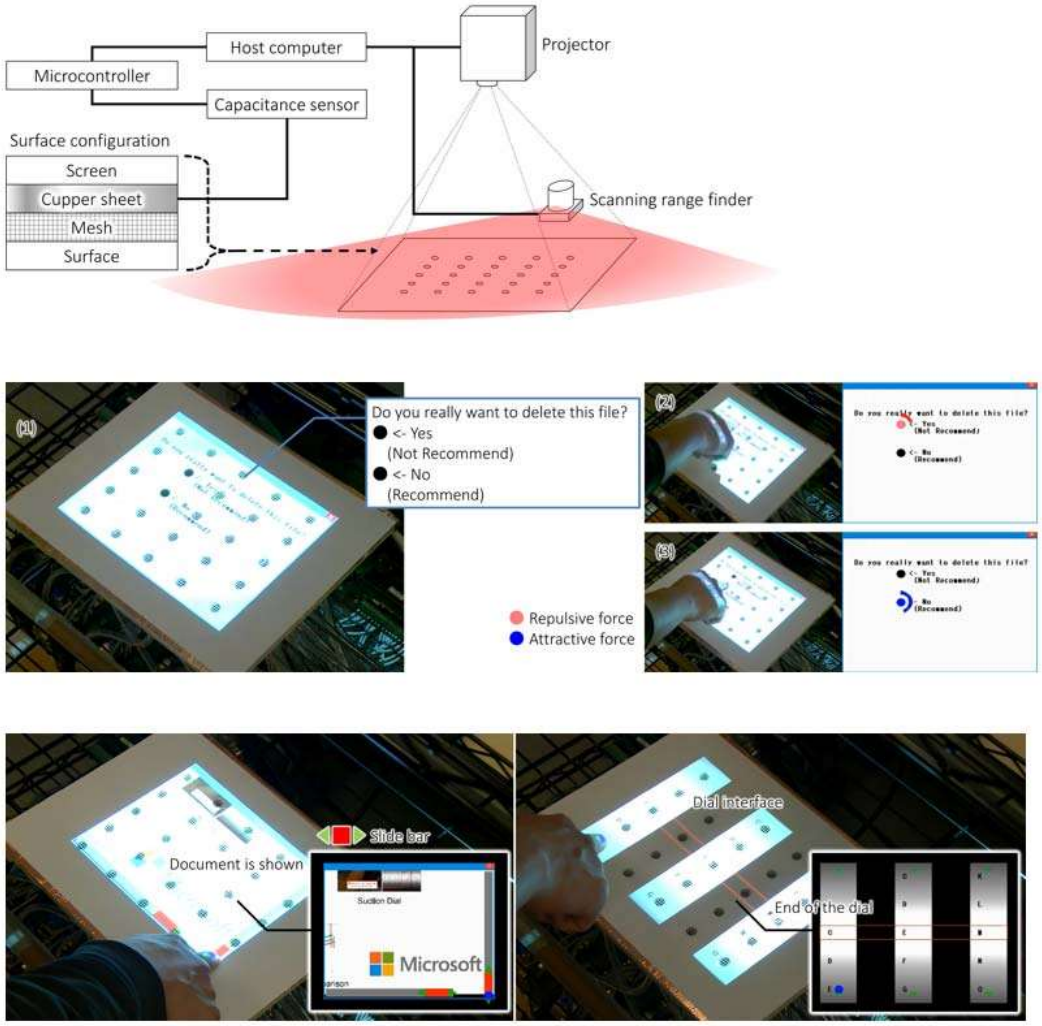

Figure 4. (top) System configuration for enhancement of GUI: a mesh sheet, cupper sheet, and screen are mounted on the surface. A scanning range finder and capacitance sensor connected to the cupper sheet measure the 2D position of a finger on the surface and detect finger contact with the surface, respectively. According to the touch event, a host computer superimposes the image on the screen and orders the microcontroller to open the valve(s). (middle) SpiroButton warns and recommends the button by providing repulsive and attractive forces. (bottom left) SuctionSlider stops the user's finger when the slider comes to the end of the document. (bottom right) SuctionDial stops the user's finger when the dial comes to the end.

Setup and procedure

As illustrated in the top-left image of Figure 5, we made five holes in a row at the center of the 200x200x50-mm ABS surface. The interval of the holes was 36 mm. There was a high-speed touch sensor (an infrared photo reflector array and induction-based touch detection unit) installed on the surface and a tact switch located on the right side of the surface. The infrared sensor was covered with ABS resin, and a thin, black plastic sheet was fixed along the touch detection unit. In this setup, while the participant's finger did not directly touch and manipulate the image of the dial menu, it allowed the participant to clearly see the numbers without occlusion.

Based on pilot studies, we decided to project two numbers of the dial and box, as indicated in the top-right image of Figure 5. The participants placed their index finger on the center of the hole, dragged it to the center of the left hole, and released it to increase the number of the dial. They were asked to determine the maximum number of the dial (the end of the dial). When they identified the maximum number entered in the box, they pushed the switch to complete the task. They were asked to perform the task as quickly as they could. In this setup, the participants did not flick their finger; rather, they dragged it to the hole. Further, the end of the dial could not be seen until it came to the box. This setup allowed for simulating the issue of the dial interface, where it is difficult to know where the end of the dial is in a laboratory experiment setting.

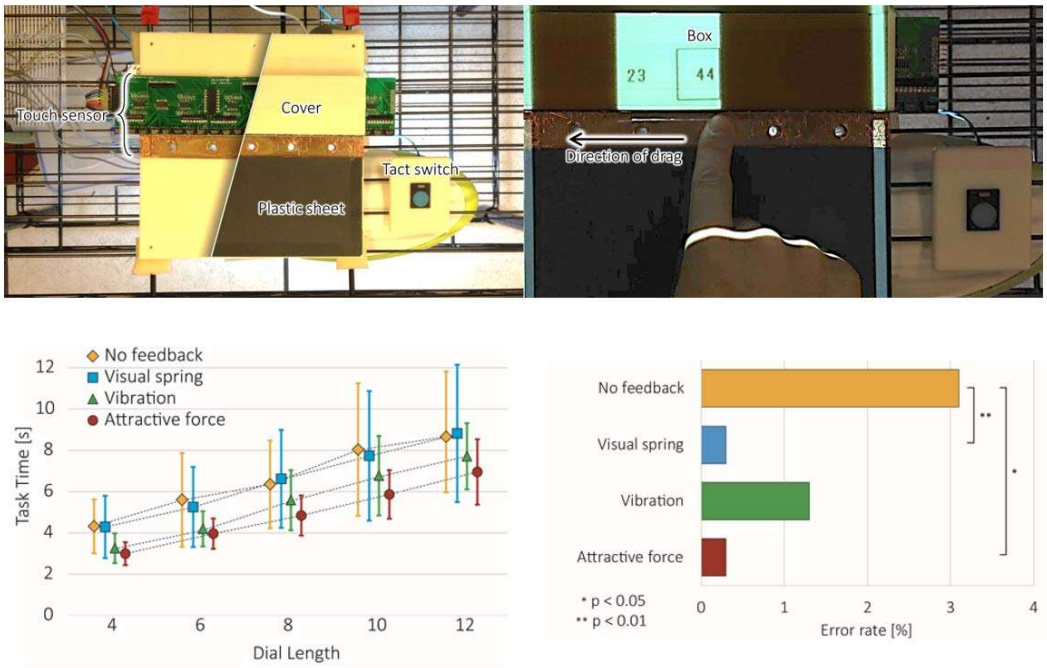

Figure 5. (top left) Experimental setup: the high-speed touch sensor (an infrared photo reflector array and an induction-based touch detection unit) installed on the surface and the tact switch located on the right side of the surface. The sensor was covered with ABS resin, and the thin, black plastic sheet was fixed along the touch detection unit. (top right) Experimental setup with two numbers of the dial projected. (bottom left) Task times for the four feedback conditions (+/- standard deviation of the mean). (bottom right) Error rates for the four conditions.

We presented five lengths of dials having 4, 6, 8, 10, and 12 numbers. At the beginning of the dial, the number was always 0, and the number was incremented with a random interval when participants scrolled the dial to the left. The interval distance between the numbers was always 36 mm (the same as the distance between the holes). We presented four conditions. The first condition was attractive force (AF), where the attractive force was provided from when the end of the dial came to the box to when the finger was released. The second condition was no feedback (NF), where the image of the dial became frozen when the end of the dial came to the box. The third condition was visual spring (VS), where the image of the dial could be moved by dragging, even when the end of the dial passed through the box. This allowed participants to see a blank space after the end. When participants released their finger, the end of the dial returned to the box. The fourth condition was vibration (VB), where vibration was provided by a vibration motor installed under the surface at the same time as AF.

Twenty-four people (20 males and four females; age 20 to 28; all right-handed) participated in the experiment. The experiment had 20 (four feedbacks × five dial lengths) conditions. The experiment consisted of four blocks. One feedback condition was assigned to one block. One block consisted of two sections: one where the participants practiced the task 15 times (the five lengths of the dials were randomly presented three times), and the other where they conducted the task

15 times with assigned feedback. The participants conducted all four blocks. The order of the blocks (feedback conditions) was counterbalanced within the participants. We collected the data (task completion time and error number) only from the latter sections. During the experiment, white noise was played through earphones to mask the audio cues produced by the attractive force and the vibration feedback.

Result

The mean task times for the four feedback conditions with respect to the five dial lengths are displayed in the bottom-left image of Figure 5. A two-way within-participants repeated-measures analysis of variance (ANOVA) was performed on the task time data. The within-participants factors were dial length (L4, L6, L8, L10, and L12) and feedback (NF, VS, VB, and AF). There were significant main effects for dial length ($F(4, 92) = 185.3$; $p < 0.001$; $\eta_G^2 = 0.3908$) and feedback ($F(3, 69) = 14.7$; $p < 0.001$; $\eta_G^2 = 0.1137$). Multiple comparison tests (Bonferroni test) for feedback indicate significance in the task time (AF < VB < NF = VS; $p < 0.05$; alpha level = 0.0083). The interaction effect for dial length × feedback was not significant, although it demonstrated a certain trend toward significance ($F(12, 276) = 1.7$; $p = 0.075$). To determine the trend, we performed multiple comparison tests for feedback at each dial length with a 0.05 significance level and a 0.0083 alpha level. At L4 and L6, there were significances other than between VB and AF and between NF and VS (meaning there was significance between with and without haptic feedback conditions). Moreover, there was no significance between NF and VB at L8, no significance between VS and VB at L10, and no significances between NF and VB or between VS and VB at L12. Conversely, there were significances between NF/VS and AF at all conditions of dial length. These results indicate that the AF encouraged reducing the task time even when the dial length was long. One possible reason could be that the participants attempted to repeat the scrolling gesture. Even if the vibration was present, they ignored or missed the vibration because they attempted to scroll faster to reach the end of the dial when they could not find it with the initial few scrolls. This would seldom occur in AF because AF had the participants stop their fingers at the end of the dial, which allowed them to move their finger quickly toward the switch.

The error rates for the four feedback conditions are displayed in the bottom-right image of Figure 5. A binomial logit model analysis was performed on the error rate data. The following model was applied:

$$Error \sim \alpha + \beta \times FDBK + r, \tag{5}$$

where *Error* is a rate of error, *FDBK* are the feedback conditions (NF, VS, VB, and AF), and r is the random effect (participant). When NF was set as a baseline, the odds ratios of VS, VB, and AF were 0.067 ($p < 0.01$), 0.411 ($p = 0.07$), and 0.202 ($p < 0.05$), respectively, which indicates that AF and VS significantly reduced the error.

In summary, AF was the best feedback condition in terms of reducing task time and rate of error. One reason could be that AF can intervene directly in a user's motion, which offers intuitive interaction similar to a mechanical dial on a touch screen.

Deformation of Soft Object

To demonstrate deforming a soft object on SpiroSurface, we developed two systems. One folds a piece of cloth that does not have any actuator or special component to receive forces, such as a self-assembly robot or magnetic system. The other is a 5x5 segment display with three states using a rubber surface. Both reflect the potential of our approach to deform soft objects.

Cloth folding

To fold a piece of cloth, it must be bent at the center and one side must be moved over to the other side. To achieve this, the force display must apply moments to the cloth. As described, the display can generate both repulsive and attractive forces on the surface. Using this capability, we

used the following approach, as indicated in the left image of Figure 6. The system fixes the center of the cloth by generating an attractive force, which becomes a fulcrum. Repulsive force is then applied to one side of the cloth, which generates moments, and the cloth is folded in half.

The right image of Figure 6 displays capture images from the video recorded during the folding of a piece of cloth. Repeating a similar procedure, the force display succeeded in folding the cloth in quarters. Although timing and position of the force profiles were manually defined, this could be automatic by recognizing the shape of the cloth with a camera and creating a sophisticated algorithm. Although a surface that can only fold a cloth is not practical, it demonstrates the potential of the application of SpiroSurface—the ability to manipulate an object without an active actuator. Further, if the spatial and temporal resolution is improved, the surface could manage multiple objects.

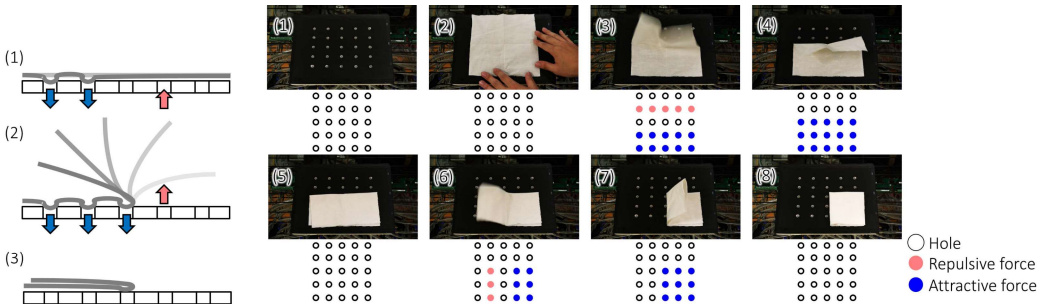

Figure 6. (left) Illustration of generating moment to a piece of cloth: (1) providing attractive force at the center of the cloth, (2) pushing one side of the cloth, and (3) moving one side over to the other. (right) Folding a piece of cloth in quarters: (1-2) placing the cloth, (3-5) folding the cloth in half, and (5-8) folding the cloth into quarters.

Three-state 5x5 segment rubber display

The top-left image of Figure 7 presents the setup for the three-state 5x5 segment rubber display. It consists of SpiroSurface, a rubber plate with 25 chambers, and a video projector. We created the rubber plate from a sheet of silicone rubber and partitioned it with acrylic plates and double-sided tape for the silicone rubber. We designed the plate to fit the developed SpiroSurface; hence, the size of the chamber and rubber plate were 156x156 mm and 24x24 mm, respectively (see the top-right image of Figure 7). The rubber plate was fixed on the surface with double-sided tape to prevent air leaks. We used the projector to ensure that the display contrast was high.

The bottom-left image of Figure 7 illustrates the rubber plate displaying characters ("+," "X," and "A") by making them concave. This is achieved by providing attractive forces at appropriate holes. Because each chamber is independently sealed, providing an attractive force from one hole deflates the rubber above the hole.

Providing a repulsive force can inflate the rubber. As indicated in the bottom-right image of Figure 7, a geometric convex can be displayed (a convex surrounded by eight concaves), which demonstrates how the display can offer three bumpiness states (flat, convex, and concave). Switching bumpiness with minimal frequency can express heartbeat-like motion, which can be touched by the user. Compared to directly touching the hole on a rigid surface, the rubber display offers a soft sensation to users, which we expect will provide affective tactile sensations.[9]

Although the current prototype offers only on/off control of both forces, the resolution of inflation or deflation can be increased by controlling the intensity of the force, such as pulse-width modulation control with high-speed valves.

Three DoF Rotation Control of Object

This section describes three DoF rotation control of an object on the surface. The top-left image of Figure 8 illustrates the setup for demonstrating three DoF rotation control (pitch, roll, and

yaw) of an object on the surface. We employ an augmented-reality (AR) scenario where a physical object (a small representation of an airplane) interacts with a projected virtual world (aerial map). The system consists of the surface, screen extension (897x445 mm), plane-shaped polystyrene foam plate with an AR marker, projector, camera, and force-moment converter. The projector is used for superimposing the images of the virtual aerial map and plane on the physical surface and the plate, respectively. The camera is used for tracking the AR marker to measure the pitch, roll, and yaw angles of the plate. Depending on the angle, the direction of scrolling the map (position of the plane in the virtual world) and rate of magnification of the map (altitude of the plane in the virtual world) can change.

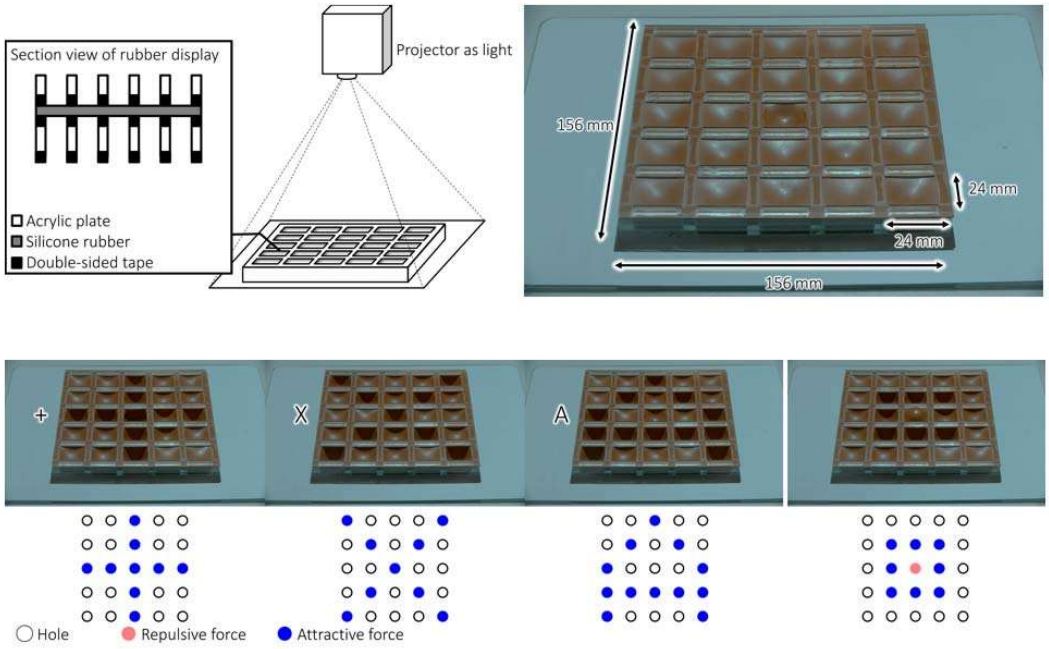

Figure 7. (top left) Configuration of three-state 5x5 segment rubber display. (top right) Display. (bottom left) Displaying characters by creating concaves with attractive force ("+," "X," and "A"). (bottom right) Creating bumpiness (a convex surrounded by eight concaves).

The top-right image of Figure 8 displays the structure of the converter. The converter consisted of a pivot and rotational disk made of ABS resin. The ball joint of the pivot was covered with silicone oil to smoothly rotate the disk, and the bottom was fixed to the surface. Providing a repulsive force can generate moments about the x and y axes (roll and pitch rotation).

To generate moments about the z-axis (yaw rotation), the disk had two cone-shaped holes. When the yaw angle of the plate was zero degrees and a repulsive force was applied to the slope of the cone, the disk rotated until the hole providing the repulsive force and the hole of the cone became concentric. Because changing the hole(s) provided repulsive force, the plate could be rotated 360 degrees about the z-axis. The holes providing the repulsive force were determined by the yaw angle measured by the AR marker and camera.

The middle-left and middle-right images of Figure 8 indicate the yaw and pitch rotation of the plate, respectively. According to yaw rotation, the direction of the map's scrolling was changed to represent the travel direction of the plane. According to pitch rotation, the map was magnified for representing the altitude of the plane. Furthermore, the bottom image of Figure 7 indicates that the plane vibrated while going through a cloud. The vibration was generated by switching direction of the roll rotation.

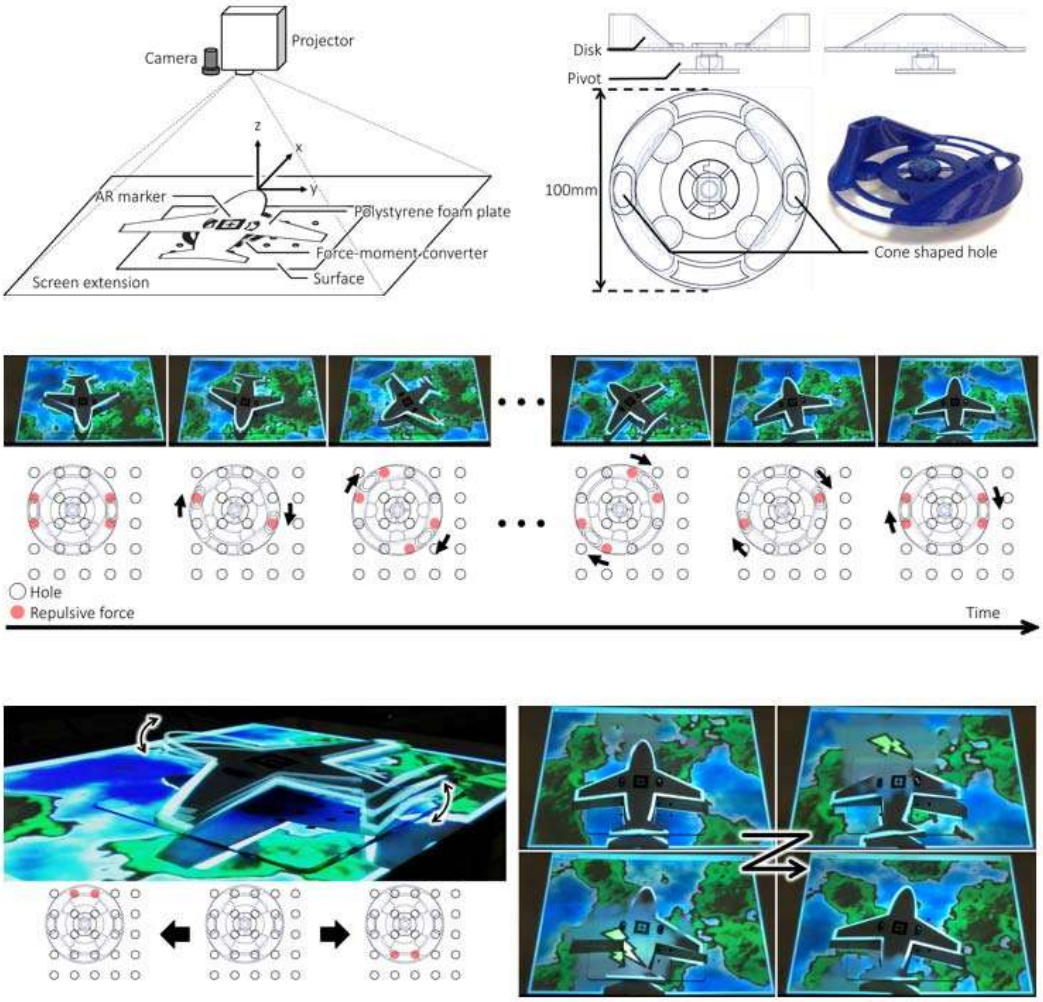

Figure 8. (top left) Configuration of three DoF rotation control for AR setup. (top right) Structure of a force-moment converter. (middle left) Yaw rotation. (middle right) Pitch rotation. (bottom) Vibrating the plane (roll rotation) while the plane is going through a cloud.

DISCUSSION

Advantages

This section describes the advantages of SpiroSurface as a force display for interactive tabletops compared with other force displays. The major advantages are that it provides force in two directions, offers interactions to the user without attaching or holding additional devices, and deforms and moves physical widgets without embedding an additional active component.

Follmer *et al*. developed inFORM, a shape display for interactive tabletops using arrays of plastic pins.[5] The display can manipulate objects and interact with users on the surface. Although inFORM has a higher spatial resolution than SpiroSurface and can actively push objects and users, it cannot actively pull them.

Electrostatic actuation is one method of generating an attractive force and is used to represent friction on the surface. Bau *et al*. developed TeslaTouch, which controls electrostatic friction between the surface and the user's finger.[10] Although it is possible to provide an attractive force

without requiring the user to hold an additional device, the sensation is only felt while a finger is moving on the surface. Furthermore, it is difficult to provide the force in two directions.

Weiss *et al*. developed Madgets[3] and FingerFlux,[4] which actuate magnets embedded in physical widgets and attached to a user's fingers using a magnetic force provided by the surface consisting of arrays of electromagnets. Switching polarity of the electromagnets provides repulsive and attractive forces, and embedding magnets allows the driving of the widgets. However, the user must attach the magnet to the finger to experience force interaction.

Pneumatic systems have been used as force displays for interactive tabletops. For example, Suzuki and Kobayashi established a 3D visual and haptic interactive system with 100 air-jet nozzles, where the user interacts with a stereoscopic image with a stick.[2] Hoshi *et al*. developed a tactile feedback device using an array of ultrasonic speakers.[1] By precisely controlling the phase of waveform output from ultrasonic speakers, the device can provide tactile feedback in the air (above the surface) without holding or attaching a device. Although these displays can provide repulsive force in the air, they do not address attractive forces. Yamaoka *et al*. conducted basic research for developing a tactile display that presents various stickiness sensations using air suction.[11] We developed VacuumTouch, which is an attractive force display for interactive tabletops using air suction.[6] SpiroSurface combines air blowing with the VacuumTouch architecture for achieving a force display that can provide both repulsive and attractive forces. This approach expands the freedom of the interaction design as demonstrated earlier. Furthermore, we demonstrated that SpiroSurface can offer three DoF moment of objects using the developed force-moment converting mechanical component.

Limitations and Possible Improvements

The prototype in this study has several limitations. One is that the force cannot be provided for a long time if the object or finger does not completely cover the hole(s) on the surface. This can be solved using a compressor/vacuum with a higher flow rate or larger air tanks to maintain the air pressure. The current solution is to limit the duration of opening valves.

Additionally, the current system requires approximately 50-400 ms to generate and dissipate the forces, which can be perceived by human users. Although the latency did not deteriorate the performance of any specific GUI task, human users generally prefer low-latency feedback. Further, the developed display cannot control the intensity of the force using PWM scheme because of the latency. Through both theoretical and experimental evaluation, we determined that one main factor of the latency in the developed display is the response time of the air valves. The driving power of the solenoid depends on the current. Thus, applying overdriving current to the coil of the valve or using a low voltage-rated solenoid are both possible solutions. As expected, the high pressure applied to the valve influenced the reaction time of the valve. The high pressure helps with opening the valve, whereas it impeded closing the valve. A solution to reduce the effect of the pressure is employing another type of the valve such as a spool type. Another factor is airflow path. A possible solution for reducing the latency is making the diameter and length of the tube thicker and shorter, respectively. However, the effect of this solution could be significantly less than that of employing the high-speed valve mentioned earlier. The solution would be more effective if the display employed low pressure.

Unlike ultrasonic[1] and magnetic[3,4] force, it is difficult for SpiroSurface to provide a force, especially an attractive force, with the object above the surface. Using a more powerful compressor or pump could possibly offer the force at a greater distance. However, controlling spatial resolution (position and range of force) would remain difficult.

The current system has a low spatial resolution of force provision (smaller number of holes per area and large holes), which limits the potential applications and occludes the visual image. Further, although the surface is used as a haptic interface, the holes produce unnecessary haptic cues with the edge even when the air valve is closed and the surface is covered with a mesh screen. This can be solved in the future by implementing micro-electro-mechanical systems (MEMS) technology such as a micro-valve and microchannel. Moreover, using MEMS technology allows for creating a surface that includes an MEMS-based visual display.[12]

CONCLUSION

This article presents SpiroSurface, a novel force display for interactive tabletops. SpiroSurface uses a pneumatic system to generate both repulsive and attractive forces. Users can feel the force from the display without holding or attaching additional devices. Furthermore, the shape and motion of the object on the surface can be manipulated without embedding additional actuators in the objects. Using these unique capabilities, we demonstrated several interactive tabletop applications of SpiroSurface, combining video projections and motion trackers. The applications included enhancement of GUI, deformation of soft objects, and three-DoF rotation control of objects. The current force display has several limitations, including low spatial, temporal, and force output resolutions. We expect that introducing MEMS technology can overcome these limitations, which we believe expands the potential of the pneumatic system as a force display.

SIDEBAR: BACKGROUND AND RELATED WORK

Research and design in the field of haptic interfaces for interactive surfaces, such as mobile screens and tabletop screens, has been growing. Because touch screens themselves do not have a mechanical button, vibration feedback improves user performance, such as selecting and clicking visual widgets on a screen.[13,14] Furthermore, the haptic interface also enriches the realism of the visual environment. For example, a user can perceive the texture or material of an image.[15,16] To expand the range of expression, researchers have been exploring novel technologies for developing haptic displays and measuring users' behavior on the surface.

In this article, we categorize haptic displays into three groups: (1) lateral force, (2) repulsive force, and (3) attractive force. A force display can guide the user's hand to the desired position and assure its manipulation. Lateral force displays generate the force in a direction tangent to the surface.[17,18] Saga and Deguchi, for example, developed a lateral-force-based haptic interface for touch screens employing motors and wire strings that pull the user's finger from the corners of the screen.[17] Repulsive force displays generate the force in a direction from the surface towards the space above the surface. A repulsive force is frequently used for simulating mechanical-button clicking on the surface.[13,14] Attractive force displays generate a force in a direction opposite to a repulsive force. For example, Weiss *et al*. developed FingerFlux, which attracts the user's finger to the surface with a permanent magnet attached to the finger and electromagnetic actuation.[4] Recent haptic interfaces actuate devices attached to the user, object, or surface. The last option allows the user to easily experience direct touch interaction with the surface because they are not required to hold or attach an extra device.

From this background, we developed VacuumTouch, a force display for interactive tabletops, which generates an attractive force using air suction. VacuumTouch offers direct touch interaction without requiring users to hold or wear additional devices.[6] A primary reason for focusing on attractive force was that previous work suggested that it can guide users to a desired position on the surface.[4,6,19] Although these works quantitatively demonstrated that the attractive force assisted the users' task, both displays used electromagnetic power, which requires the users to attach or hold additional devices. In addition to the improvement of a user's task performance, an attractive force can simulate variable stickiness,[11] which implies that the attractive force can expand the range of expression on the interactive tabletop.

Pneumatics-based force displays that provide repulsive force sensations have also been developed. To our knowledge, an early repulsive pneumatics-based force display was Heilig's Sensorama,[20] which is accepted as being one of the first immersive VR systems; it provides tactile sensation using a fan. Because fans are cost- and power-efficient, they are implemented in many VR systems. BYU-BYU-View is an example of a pneumatic-based display for interactive surfaces where users interact with the projected image on a surface that can sense the user's huffing and provide wind from DC fans.[15] Another display employs an array of ultrasonic speakers.[9] By precisely controlling the phase of the waveform output from the ultrasonic speakers, the device can provide a force in the air (above the surface) without holding or attaching a device. An air vortex is another technique for providing repulsive force in the air from the surface.[21] Hashimoto *et al*. developed a haptic display that employs audio speakers.[9] The user holds the speakers in

hand while the speaker vibrates the air between the speaker cone and their palm. When the frequency is extremely low (such as 1 Hz), they feel both a repulsive and attractive force. The employment of air compressors and air valves has also been explored. Gwilliam *et al*. developed a 3D haptic display using an air-jet, which renders the 3D shape of a lump on the user's finger.[22] Suzuki and Kobayashi established a 3D visual and haptic interactive surface with 100 air-jet nozzles, where the user interacts with a stereoscopic image with a stick.[2] The nozzles connect to an air compressor through electric valves that control the output air and blow air to the stick, which results in repulsive forces representing the 3D shape. As with attractive force displays, repulsive force displays provide a wide range of experiences through the air.

ACKNOWLEDGMENTS

We thank Zhaoyuan Ma for his great help with the development of our prototype system.

REFERENCES

1. T. Hoshi et al., "Noncontact Tactile Display Based on Radiation Pressure of Airborne Ultrasound," *IEEE Transactions on Haptics*, vol. 3, no. 3, 2010, pp. 155–165.
2. Y. Suzuki and M. Kobayashi, "Air Jet Driven Force Feedback in Virtual Reality," *IEEE Computer Graphics and Applications*, vol. 25, no. 1, 2005, pp. 44–47.
3. M. Weiss et al., "Madgets: Actuating Widgets on Interactive Tabletops," *Proceedings of the 23nd Annual ACM Symposium on User Interface Software and Technology* (UIST), 2010, pp. 293–302.
4. M. Weiss et al., "FingerFlux: Near-Surface Haptic Feedback on Tabletops," *Proceedings of the 24th Annual ACM Symposium on User Interface Software and Technology* (UIST), 2011, pp. 615–620.
5. S. Follmer et al., "inFORM: Dynamic Physical Affordances and Constraints through Shape and Object Actuation," *Proceedings of the 26th Annual ACM Symposium on User Interface Software and Technology* (UIST), 2013, pp. 417–426.
6. T. Hachisu and M. Fukumoto, "VacuumTouch: Attractive Force Feedback Interface for Haptic Interactive Surface using Air Suction," *Proceedings of the SIGCHI Conference on Human Factors in Computing Systems* (CHI), 2014, pp. 411–420.
7. W.R. Ferrell, "Delayed Force Feedback," *Human Factors*, vol. 8, no. 5, 1966, pp. 449–455.
8. E.E. Topçu, I. Yüksel, and Z. Kamış, "Development of Electro-Pneumatic Fast Switching Valve and Investigation of its Characteristics," *Mechatronics*, vol. 16, no. 6, 2006, pp. 365–378.
9. Y. Hashimoto, S. Nakata, and H. Kajimoto, "Novel Tactile Display for Emotional Tactile Experience," *Proceedings of the International Conference on Advances in Computer Entertainment Technology* (ACE), 2009, pp. 124–131.
10. O. Bau et al., "TeslaTouch: Electrovibration for Touch Surfaces," *Proceedings of the 23nd Annual ACM Symposium on User Interface Software and Technology*, 2010, pp. 283–292.
11. M. Yamaoka, A. Yamamoto, and T. Higuchi, "Basic Analysis of Stickiness Sensation for Tactile Displays," *International Conference on Human Haptic Sensing and Touch Enabled Computer Application*, 2008, pp. 427–436.
12. I. Bita, A. Govil, and E. Gusev, "Mirsol(R) – MEMS-Based Direct View Reflective Display Technology," *Handbook of Visual Display Technology*, 2012, pp. 1777–1786.
13. M. Fukumoto and T. Sugimura, "Active Click: Tactile Feedback for Touch Panels," *Extended Abstracts on Human Factors in Computing Systems*, vol. CHI'01, 2001, pp. 121–122.
14. I. Poupyrev and S. Maruyama, "Tactile Interfaces for Small Touch Screens," *Proceedings of the 16th Annual ACM Symposium on User Interface Software and Technology* (UIST), 2003, pp. 217–220.
15. E. Sawada et al., "BYU-BYU-View, a Wind Communication Interface," *ACM SIGGRAPH 2007 Emerging Technologies*, 2007, p. 1.

16. T. Hachisu and H. Kajimoto, "HACHIStack: Dual-Layer Photo Touch Sensing for Haptic and Auditory Tapping Interaction," *Proceedings of the SIGCHI Conference on Human Factors in Computing Systems* (CHI), 2013, pp. 1411–1420.
17. S. Saga and K. Deguchi, "Lateral-Force-Based 2.5-Dimensional Tactile Display for Touch Screen," *IEEE Haptics Symposium* (HAPTICS), 2012, pp. 15–22.
18. D. Wang et al., "Haptic Overlay Device for Flat panel Touch Displays," *IEEE Haptics Symposium* (HAPTICS), 2004, p. 290.
19. M. Akamatsu and S. Sato, "A Multi-Modal Mouse with Tactile and Force Feedback," *International Journal of Human-Computer Studies*, vol. 40, no. 3, 1994, pp. 443–453.
20. M. Heilig, *Sensorama simulator*, US Patent 3050870, 1962.
21. R. Sodhi et al., "AIREAL: Tactile Gaming Experiences in Free Air," *CM Transactions on Graphics (TOG)*, vol. 32, no. 4, 2013.
22. J.C. Gwilliam et al., "Characterization and Psychophysical Studies of an Air-Jet Lump Display," *IEEE Transactions on Haptics*, vol. 6, no. 2, 2013, pp. 156–166.

ABOUT THE AUTHORS

Taku Hachisu is a researcher at the University of Tsukuba. He has a PhD in engineering from the University of Electro-Communications. His research interests include augmented/virtual reality, haptics, human-computer interaction, and wearable devices. He is an ACM member. Contact him at hachisu@ai.iit.tsukuba.ac.jp.

Masaaki Fukumoto is a lead researcher at Microsoft Research. He has a PhD in engineering from the University of Electro-Communications. His research interests include portable and wearable interface devices. He is an ACM member. Contact him at fukumoto@microsoft.com.